Asian Journal of Chemistry; Vol. 37, No. 3 (2025), 624-632

ASIAN JOURNAL OF CHEMISTRY

https://doi.org/10.14233/ajchem.2025.33276

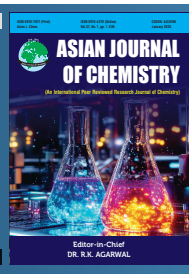

Potential of Novel Synthesized Neem Gum and Gelatin Biocomposites based Topical Gel in Effective Wound Healing

SONIA ARORA[1,2], MALKIET KAUR[3], AMARJOT KAUR GREWAL[1], SAMRAT CHAUHAN[1], MANDHEER KAUR[2] and MANJU NAGPAL[1,*]

[1]Chitkara College of Pharmacy, Chitkara University, Rajpura-140401, India
[2]Chandigarh College of Pharmacy, Chandigarh Group of Colleges, Landran-140307, India
[3]M.M. College of Pharmacy, Maharishi Markandeshwar (Deemed to be University), Mullana-133207, India

*Corresponding author: E-mail: manju.nagpal@chitkara.edu.in

Received: 26 December 2024; *Accepted*: 4 February 2025; *Published online*: 28 February 2025; AJC-21919

Wound healing and tissue repair is a complex cascade evolving due to anthropogenic and lifestyle factors. For this purpose, a well-orchestrated wound dressing can help to cover the wound or injury, which protect from surrounding environment and also provide moisture for tissue regeneration. Antimicrobial resistance is one of the major factors in increasing mortality due to wounds. Wound infection is the cause of more than 75% death in post operative infections. The biocomposites of neem gum and gelatin were prepared using crosslinking *via* pH change method and characterized with Fourier transmission infrared (FTIR), scanning electron microscopy (SEM) and X-ray diffraction (XRD) techniques. The optimized biocomposite formulation was used to formulate solid dispersions of pure drug clindamycin phosphate. The characterization studies confirmed the absence of drug-biocomposite interactions. The *in vitro* dissolution studies were carried out to evaluate the effect of amount on biocomposites polymer on the release of clindamycin from the dispersions. The optimized dispersion was incorporated into topical gel and the gel formulation exhibited sustained relese of drug for 24 h. The formulated biocomposites functioned as sustained release polymers and were employed to prolong medication release in wound healing applications.

Keywords: Biocomposites, Wound healing, Cross-linking, Sustained release, Dispersion.

INTRODUCTION

Wound healing is a dynamic and complex biological process involving hemostasis, inflammation, proliferation and tissue remodeling. In other words, it is the biological method of treatment to recover the structure and role of injured skin [1,2]. However, frequent techniques in this procedure are not respectable because they involve contraction or lead to unhygienic scars. Traditional wound dressings have some drawbacks due to bacterial invasion and adhesion, poor permeability and biodegradability, causing a long healing process [3-5]. Nowadays, biocomposites have attracted extra attention from researchers since they can provide an advantage in both medical and biological applications due to their biocompatibility and ecofriendly properties [6-8]. The popularity of biomaterials has increased due to many characteristics that involve supplying clean and easily soluble gum with water solubility to be used as a thickening and stabilizing ingredient in food, drugs and cosmetics, depending on its ability to speed up the healing of small wounds, due to being a good emulsifier of pharmaceuticals. Among various materials, biocomposites derived from natural polymers have emerged as promising candidates due to their biocompatibility, biodegradability and cost-effectiveness [9,10].

Neem gum, a natural exudate from the *Azadirachta indica* tree, is a well-established biomaterial known for its antimicrobial, anti-inflammatory and antioxidant properties, which are critical for promoting wound healing [11]. It is a non-ionic polymer with a lower molecular weight of around 221 to 249 kDa. Neem gum steadily dissolves in water and has demonstrated its potential in assisting the release of bioactive agents from mucoadhesive preparations across the cell monolayer in buccal mucosa. This non-ionic bioactive biopolymer, with excellent emulsification and rheological data, having broad water retention and hydrophilicity, proved fruitful for nanoinclusions as a stable drug delivery system in the process of engrossing the drug for tissue regeneration [11,12].

Gelatin, a natural polymer obtained from collagen, complements neem gum's properties due to its excellent biocompatibility, bioactivity and ability to form hydrogels or films suitable for wound dressing applications. Gelatin-based biocomposites have been extensively studied for their ability to enhance cellular proliferation, moisture retention and overall wound repair [13,14]. Polymeric based neem gum biocomposites offer unique advantages, such as controlled drug release, antimicrobial activity and enhanced mechanical properties, making them suitable for chronic and acute wound healing [15]. Furthermore, such biocomposites can be functionalized with therapeutic agents or nanoparticles to further enhance their efficacy. As natural and biodegradable materials, neem gum and gelatin also provide an ecofriendly and cost-effective alternative to the synthetic wound dressings, addressing the limitations of conventional treatments [11].

The main objective of the present work is to design the neem gum and gelatin biocomposites based topical gel with encapsulation of the antibiotic drug clindamycin phosphate for effective wound healing. It is the exploration of bioactive polysaccharides to develop topical gel by preparing biocomposite neem gum and gelatin to develop materials of choice wherein the wound fluid sorption capacity could be controlled by controlling the network density of the topical gel by varying biomaterial and crosslinker contents.

EXPERIMENTAL

Clindamycin phosphate was obtained as gift sample from Hufort Healthcare Pvt Ltd., Mumbai, India. Neem gum was purchased from Yarrow Pharma, Mumbai, India and Gelatin from Merck Pvt Ltd., India.

Characterization: The IR spectra of clindamycin, biocomposite and solid dispersion were studied over a 4000-650 cm^{-1} frequency range with Perkin Elmer-Spectrum RX-FTIR instrument using KBr disc method. A PanalyticalXpert Pro diffractometer, was used to determine the crystallinity of clindamycin, biocomposite and solid dispersion. The XRD patterns of each sample were measured from 5-50º 2θ using a step increment of 0.0170 at 25 ºC. The surface morphology of clindamycin, biocomposite and solid dispersion was observed using SEM (Digital SEM-JSM 6100, JEOL). Using an ion sputter coated for 5 min at 20 mA, the samples were coated with a gold-palladium layer. The observation was conducted at a working distance of 10 mm and an accelerating voltage of 5 kV.

Preparation of neem gum-gelatin biocomposites: Neem gum and gelatin biocomposites was prepared *via* ionic crosslinking method. The crosslinking of gums was performed in accordance with their ionic characteristics, which were influenced by variations in the pH of the mixture [16]. The crosslinked gum mixture was separated and dried in oven at 40 ºC. For this 2% neem gum solution and 1% gelatin solution was prepared. The initial pH of the gelatin solution was measured at 6.3, which was subsequently lowered to pH 1-2 using 0.1 N HCl. It was then added to neem gum solution and stirred for 10 min and the temperature was kept at 37 ºC. Precipitation occurs while mixing, which was precipitated, filtered and dried under oven at 40 ºC.

Formulation of drug loaded solid dispersion (SD) using biocomposite as a polymer: Solid dispersions were prepared by solvent evaporation method. Pure drug clindamycin and biocomposite were mixed in different ratio of (1:1, 1:2, 1:3 and 1:4) (Table-1) in 25 mL of solvent (70% ethanol) in a round bottom flask. The solvent was evaporated under vacuum in rotary evaporator. The resultant dried solid dispersions were allowed to dry at room temperature. Finally, the dried solid dispersions were sieved through 80# mesh and stored in air tight containers at room temperature.

TABLE-1
COMPOSITION OF VARIOUS SOLID DISPERSIONS BATCHES

Formulation code	Drug (mg)	Neem gum biocomposite (mg)
A1	100	100
A2	100	200
A3	100	300
A4	100	400

***In vitro* dissolution studies:** The dialysis bag diffusion technique was used to carry out the *in vitro* drug release studies [17]. A 5 mL of phosphate buffer (pH 7.4) was used to dissolve before being added to the dialysis bags. The bags were tightly packed before being submerged in a beaker filled with 100 mL of pH 7.4 phosphate buffer. The mixture was continually swirled at 50 rpm with a magnetic stirrer while the temperature was set to 37 ºC. About 3 mL of dispersion was withdrawn and examined and drug content using UV-spectrophotometry at 238 nm at specific intervals. Fresh buffer was added to replace the volume of dispersion media to maintain sink conditions. The drug release studies were conducted in triplicate.

Preparation of topical gel incorporating solid dispersions: Carbopol 940 (1% w/v) solutions was prepared and kept to swell during all night. An optimized batch of solid dispersion (A3) was dispersed to carbopol gel with continuous stirring of 10-15 min to allow integration of carbopol gel into solid dispersion and batch was denoted as G1. Triethanolamine was added dropwise to the gel to maintain pH and Tween 80 (1%) was also added to enhance the permeation. The prepared gel formulations were kept aside for 15 min without disturbance to emit entrapped air out and were stored in tightly closed containers at room temperature for further evaluation.

Evaluation of topical gel

Physical appearance: Colour and odour was evaluated visually.

Determination of pH: It was evaluated using a digital pH meter. The pH of the gel was measured by dropping the glass electrode into the formulation.

Determination of viscosity: The viscosity of the prepared gels was determined using Brookfield viscometer by using spindle no. 64 at 10 rpm and a temperature of 25 °C.

Determination of spreadibility: It was evaluated *via* using a glass slide and wooden block apparatus. The gel formulation (1 g) was kept on a preset glass slide and another movable glass slide was placed over the first glass slide and 50 g weight was added to the slide for 5 min. The duration used for the separation

of slides was observed and measured by using the following formula:

$$S = \frac{M \times L}{T}$$

where S = spreadability (g cm/s), M = mass (g), T = time (s).

Drug content: Topical gel formulation (1 g) was weighed and dissolved in a suitable solvent. The mixture was stirred or shaken for 15-30 min, filtered and the drug content was measured using a UV-visible spectrophotometer.

***In vitro* drug release studies:** The *in vitro* dissolution studies of gel (G1) and marketed formulation (MF) were carried out on a PERMION diffusion cell apparatus. Topical gel containing drug equivalent to 100 µg were introduced into dialysis membrane pouches and kept in a beaker filled with phosphate buffer (6.8 pH) at 37 ± 0.5 ºC. Aliquots were withdrawn at the periodic intervals for 24 h and each time replaced by the same quantity of dissolution medium. Samples were analyzed spectrophotometrically at a 238 nm.

***In vitro* antimicrobial studies:** The agar plates were prepared by dissolving the agar in water and then autoclaved for 15 min at 121 ºC. Then, the agar medium was allowed to cool at 40-45 ºC and solidify it under laminar airflow. *E. coli* (Imtech strain-1687) and *Micrococcus* (Imtech strain-1430) were used to estimate the antibacterial efficacy of the topical formulations containing clindamycin phosphate. The solidified agar plates were taken and the prepared inoculums was applied by streaking method. The plates were kept to dry for 5 min at room temperature. Agar-well diffusion assay was used for studying the potential activities of the prepared biocomposites. Wells were prepared by using a sterile cork borer by making holes in the inoculated agar plates. Each well was 5 mm in diameter. A weighed amount of the formulation A4, G1 and MF was placed into each well. The plates were incubated at 37 ºC for 72 h and observed for inhibition zones. The area of the inhibition zones was measured in mm.

***In vivo* studies:** Animal research was carried out under protocols number (IAEC/CCP/22/01/PR-16) in line with guidelines approved by the Animal Ethical Committee of Chitkara College of Pharmacy, Chitkara University, Rajpura, India. Female Wistar rats, weighing 170-230 g and aged 4-6 months, were utilized to examine the efficacy of gum in the healing of *in vivo* excision wounds. The animals were housed in cages equipped with ventilation, sawdust bedding and *ad libitum* food and water and the temperature of 24 ± 1 ºC with a light/dark cycle of 12 h. During the light phase, every experiment, including surgery was conducted. As previously described [18], the study followed the excision wound healing model. The animals were anaesthetized by kitamine-xylazine cocktail (1 mg ketamine and 0.1 mg of xylazine per 10 g b.w. i.p), the mid-dorsal region of each animal's fur was shaved and sterile biopsy punches were used to generate paired wounds of 8 mm in diameter (Tejco Vision, India). The animals were randomly divided into five groups, each group having six rats. The following five experimental groups were framed: (i) Group I: Control group; (ii) Group II: Disease group; (iii) Group III: Neem gum-gelatin gel (without drug); (iv) Group IV: Gel formulation G1 group (10% w/v); and (v) Group V: Marketed formulation group (10% w/v).

The wound surface area was monitored 1, 3, 5, 10 and 15 days following surgery to evaluate wound healing. After 15 days, regenerated/healed tissues were collected and fixed in 10% neutral buffered formalin was embedded in paraffin and 8 mm slices of tissue were cut using a microtome (Senior Rotary Microtome, Model: RMT-30, Radical Instruments). On the sections, haematoxylin and eosin stains were added. Deparaffinized with xylene, rehydrated by dipping in ethanol solutions (100%, 90%, 70%, 50%) for 2 min each, washed with running water, then stained with haematoxylin for 3 sec. Sections were then stained for 5 s with eosin after excess haematoxylin was removed for 5 min under running water. After a thorough washing with water, the components were dried and mounted using DPX Mountant and coverslips (Sigma, India). Photographs of the stained slices were taken with a light microscope (Carl Zeiss Axiovert, Germany).

RESULTS AND DISCUSSION

Characterization of biocomposites

FTIR studies: The IR spectrum (Fig. 1a) shows the characteristic peaks corresponding to both gelatin and neem gum, confirming their successful combination into a cohesive biocomposite structure. The broad peak at approximately 3400 cm^{-1}, attributed to overlapping hydroxyl (-OH) and amide-A stretching vibrations, indicates significant hydrogen bonding between the polysaccharides of neem gum and the proteinaceous gelatin as shown in Fig. 1b. The hydrogen bonding plays a key role in enhancing the mechanical stability and structural integrity of the biocomposite. Amide-I peak near 1630 cm^{-1}, representing C=O stretching, is retained, while slight shifts are observed, suggesting interactions between the peptide bonds of gelatin and the functional groups of neem gum. Similarly, the amide-II peaks (~1565 cm^{-1}) is present but reduced in intensity, likely due to interactions between the N-H bending and polysaccharide chains of neem gum. The polysaccharide-associated vibrations such as C-O-C stretching around 1240 cm^{-1} are also observed, indicating the structural contribution of neem gum. As shown in Fig. 1c, these spectral changes suggest that the biocomposite formation involves strong hydrogen bonding and possibly electrostatic interactions between the two biopolymers, leading to a stable matrix.

XRD studies: The XRD patterns of neem gum in Fig. 2a show the broad and diffuse peaks, characteristic of an amorphous material. The XRD pattern of gelatin exhibits a broad peak centered at approximately 20º 2θ. This peak is associated with the semi-crystalline nature of gelatin, which arises from the partial alignment of its triple-helical structures (Fig. 2b). The semi-crystalline properties of gelatin are crucial for its mechanical strength and gelling properties. The XRD pattern of the biocomposite reveals a combination of features from both neem gum and gelatin. The broad amorphous peak of neem gum is still evident but overlaps with the semi-crystalline peak of gelatin. The intensity of the gelatin-associated peak near 20º 2θ is reduced and slightly shifted, indicating that the inter-

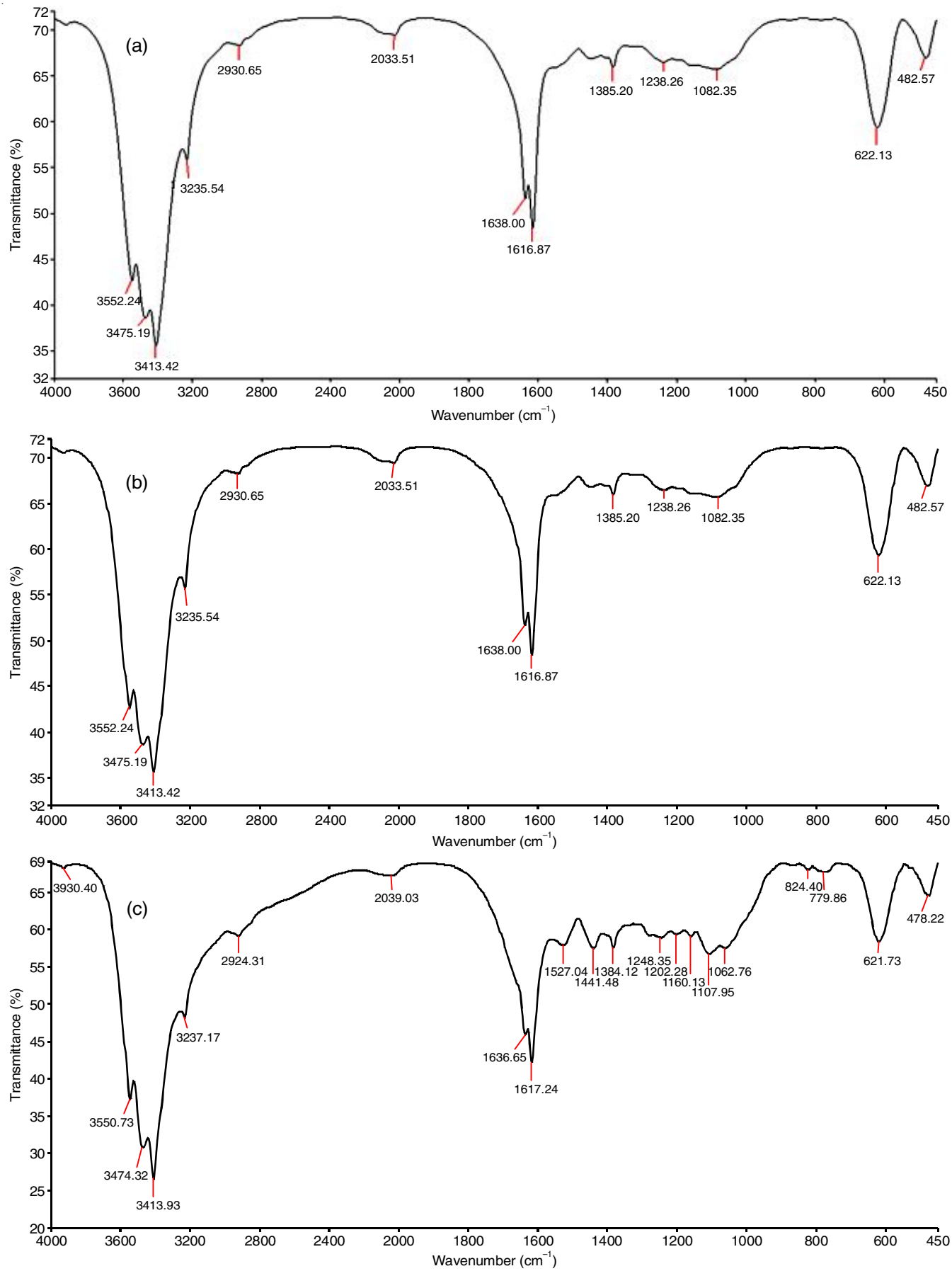

Fig. 1. FTIR spectra of (a) neem gum, (b) gelatin and (c) neem gum-gelatin composite

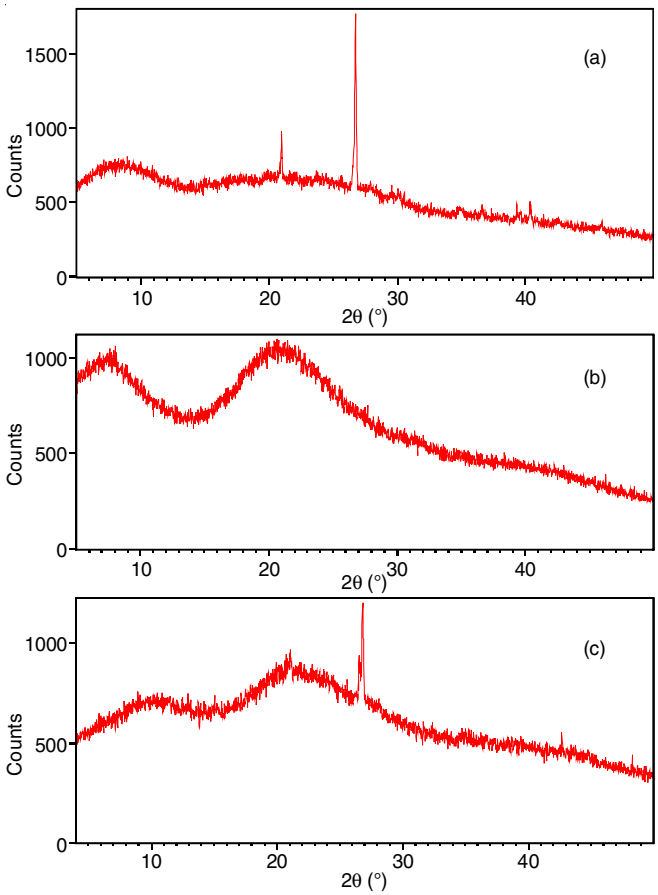

Fig. 2. XRD of (a) neem gum, (b) gelatin and (c) neem gum-gelatin biocomposite

action between neem gum and gelatin disrupts the semi-crystalline alignment of gelatin to some extent. This suggests the formation of a new structural arrangement due to the strong interactions, such as hydrogen bonding or electrostatic forces, between the polysaccharide chains of neem gum and the proteinaceous components of gelatin.

SEM studies: The SEM image of neem gum (Fig. 3a) shows an irregular, porous surface with large, jagged particles. These features are characteristic of its amorphous polysaccharide structure, which promotes its hydrophilic nature and makes it ideal for interactions with other biopolymers. The rough surface enhances its potential for physical entrapment or bonding with other materials. The gelatin image (Fig. 3b) displays a relatively smoother surface with fewer irregularities, indicating its semi-crystalline nature. The presence of folds and minor roughness suggests flexibility and elasticity, essential for its gelling and structural properties. The smoother surface compared to neem gum reflects its proteinaceous and partially ordered structure. The biocomposite image (Fig. 3c) shows a more uniform and integrated structure compared to neem gum and gelatin alone. The roughness and irregularities are reduced, indicating successful blending and interaction between neem gum and gelatin. The merged surface morphology demonstrates the formation of a cohesive matrix, likely due to hydrogen bonding and electrostatic interactions.

Formulation of solid dispersions: The solid dispersions using biocomposite as polymer were prepared and characterized.

Characterization of solid dispersions

FTIR studies: The FTIR spectrum of clindamycin phosphate (Fig. 4a) shows the characteristic peaks such as 1739.05 cm^{-1} (C=O stretching of ester groups), 1684.09 cm^{-1} (amide-I band), 1518.47 cm^{-1} (N-H bending) and 1036.20 cm^{-1} (P-O stretching, characteristic of phosphate groups. In biocomposite, the peaks correspond to the clindamycin phosphate's functional groups are retained but exhibit slight shifts or changes in the intensity. The C=O stretching (~1739 cm^{-1}) and amide-I (~1684 cm^{-1}) peaks are still present, indicating the incorporation of clindamycin phosphate. The P-O stretching peak (~1036 cm^{-1}) from phosphate groups is also retained, confirming the presence of drug in the composite. As shown in Fig. 4b. the peaks associated with neem gum and gelatin, such as -OH stretching around 3400 cm^{-1} and amide bands from gelatin (~1565 cm^{-1} for amide II, ~1240 cm^{-1} for amide III), are observed with the slight shifts, suggesting the hydrogen bonding and electrostatic interactions between the biopolymers and the drug.

XRD studies: The XRD pattern of clindamycin phosphate (Fig. 5a) exhibits sharp and intense peaks, particularly at lower 2θ values, characteristic of its crystalline nature. In the XRD pattern of drug loaded biocomposite (Fig. 5b), the crystalline peaks of clindamycin phosphate are still present but show reduced intensity and partial broadening. This indicates that the drug retains some of its crystalline structure but is partially dispersed or encapsulated within the biopolymer matrix. The

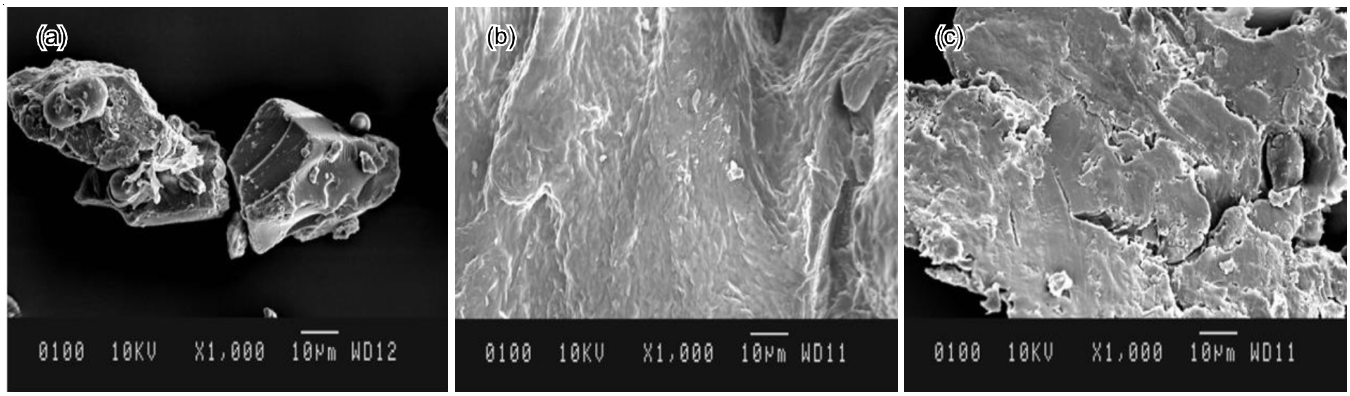

Fig. 3. SEM images of (a) neem gum, (b) gelatin, (c) neem gum-gelatin biocomposite

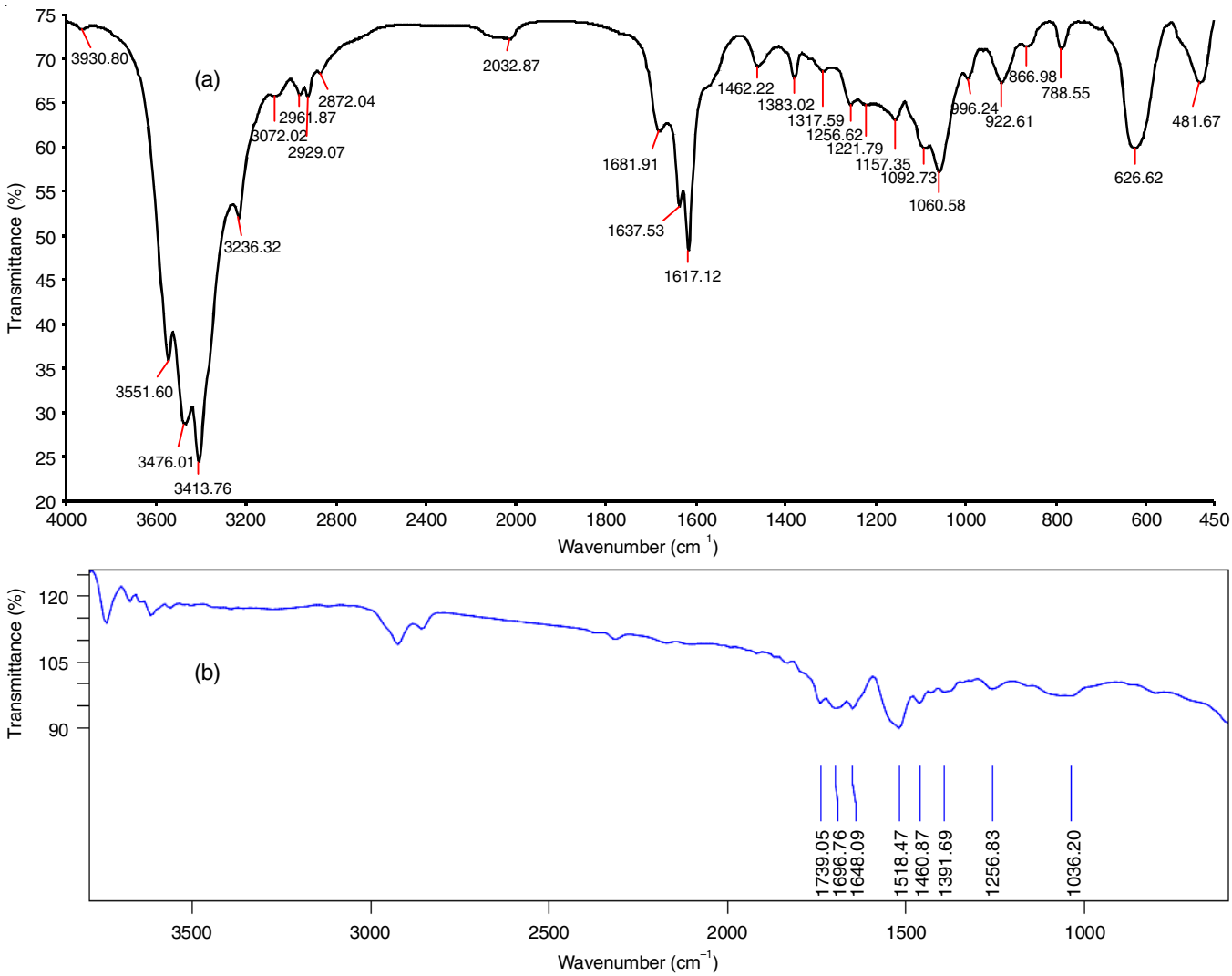

Fig. 4. FTIR spectrum of (a) clindamycin phosphate and (b) drug loaded solid dispersion formulation (A3 batch)

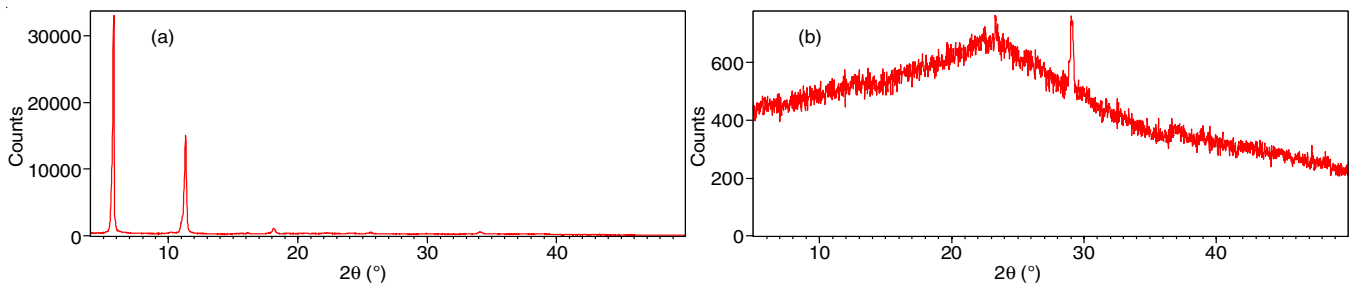

Fig. 5. XRD of (a) clindamycin phosphate and (b) drug loaded solid dispersion formulation (A3 batch)

broad amorphous halo also observed in the biocomposite, which is the characteristic of neem gum and gelatin, dominates the pattern. This suggests that the amorphous nature of the biopolymer matrix influences the crystalline structure of clindamycin phosphate, resulting in the reduced crystallinity.

SEM studies: The SEM image of clindamycin phosphate (Fig. 6a) shows a crystalline structure with sharp, well-defined edges and elongated needle-like formations. Compared to the pure clindamycin, the sharp crystalline structure of clindamycin is no longer visible. Instead, the particles appear more irregular, with rounded and aggregated shapes, suggesting that clindamycin is well encapsulated or embedded within the neem gum and gelatin matrix (Fig. 6b).

***In vitro* dissolution studies and release kinetics:** *In vitro* release profile of various solid dispersion batches (A1-A4) is shown in Fig. 7. The decrease in drug release profile is observed with the increase in composite concentration, it is due to the gel forming ability that creates a network structure, which act as a barrier to drug diffusion and slow down the release of clindamycin. Viscosity of the formulation after hydration and its swelling abilities can also be factors for sustained release. In formulation A4, it is observed that the release rate has incre-

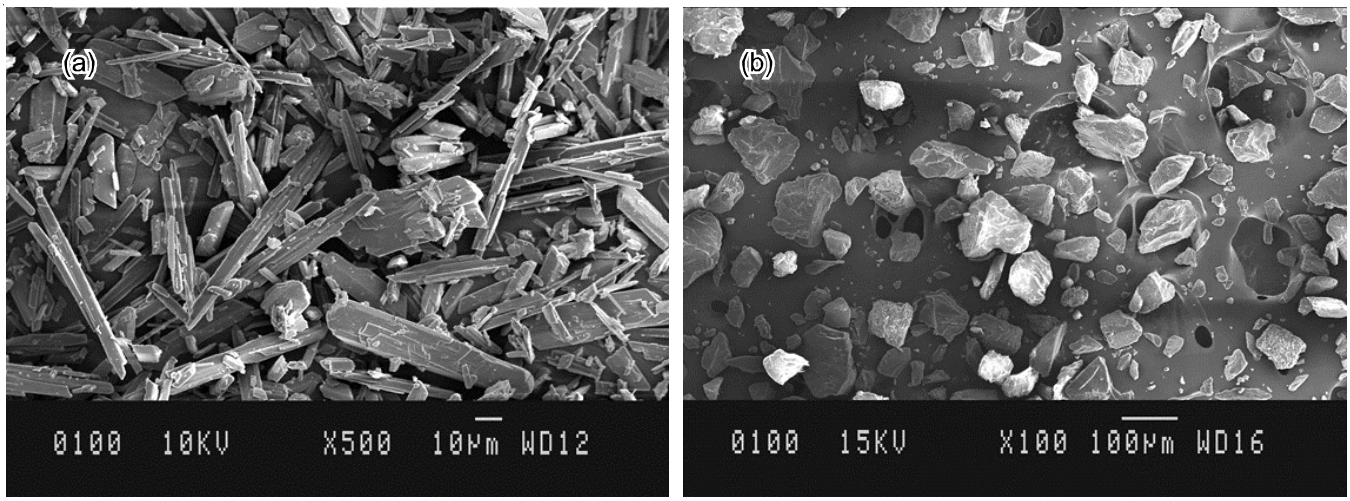

Fig. 6. SEM image of (a) clindamycin phosphate and (b) drug loaded solid dispersion formulation (A3 batch)

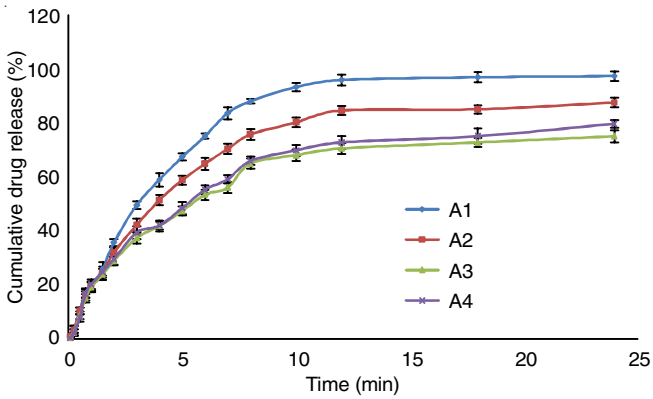

Fig. 7. *In vitro* drug release from NGC based drug dispersions (A1-A4)

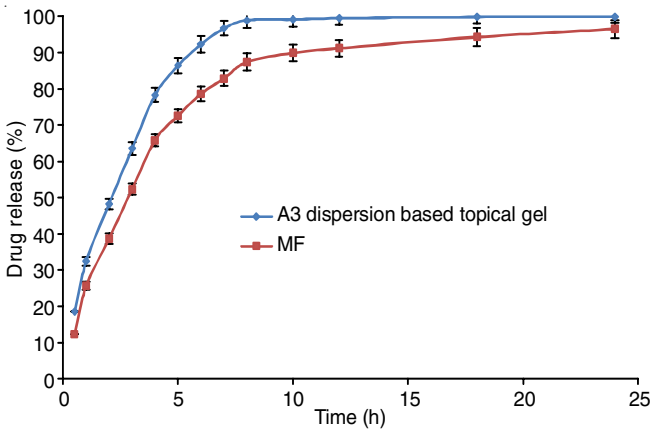

Fig. 8. *In vitro* drug release from formulated topical gel and marketed formulation

ased due to excessive swelling which has created the enlarged pores from which the drug is leaching out at faster rate. However, formulation A3 showed maximum sustained release characteristics and this formulation was selected for formulation into topical gel. The dispersions formulations exhibited higuchi release kinetic profile indicating the drug bursting out from the matrix through diffusion mechanism.

Physico-chemical parameters: The prepared topical gels were examined for various physico-chemical parameters and the results are depicted in Table-2.

***In vitro* drug dissolution release studies:** As shown in Fig. 8, formulation A3 dispersion based topical gel maintains a controlled release reaching 99.9% release in 24 h. The marketed gel achieves a slightly lower release of 96.5% after 24 h, indicating less efficient drug delivery over the extended time. The experimental formulation shows better drug dissolution and delivery through the biocomposite-based system, making it more effective for prolonged therapeutic effects.

***In vitro* antimicrobial studies:** This study highlights neem gum's potential as an antimicrobial agent, particularly for applications targeting Gram-negative bacterial infections. Neem gum demonstrates strong antimicrobial activity against *E. coli*, suggesting its efficacy against Gram-negative bacteria. Neem gum shows moderate antimicrobial activity against *Micrococcus*, indicating effectiveness against Gram-positive bacteria, but to a lesser extent compared to *E. coli*.

Percentage wound closure: In this study, *in vivo* wounds treatment with formulations healed at a considerably faster rate than the control wounds (Table-3). The groups who received formulations treatment showed a statistically significant difference from day 5 onwards and this difference remained until day 15, after the wound had formed (Fig. 9).

Histopathology studies: Histopathological analysis was carried out to compare the efficacy of wound healing in formulation A3 as compared to the normal and control group. The samples from the tissue areas of wounds at predetermined intervals were stained with hematoxylin and eosin (H&E) to visualize under a microscope. The histological analysis of the normal

TABLE-2
PHYSICO-CHEMICAL PARAMETERS OF TOPICAL GEL FORMULATION OF SOLID DISPERSION A3

Formulation code	Colour	Odour	Viscosity (cps)	Spreadibility (cm^2)	pH	Drug content
G1	White	Odourless	2643.34	3.22 ± 0.66	5.7 ± 0.8	95.54 ± 1.8

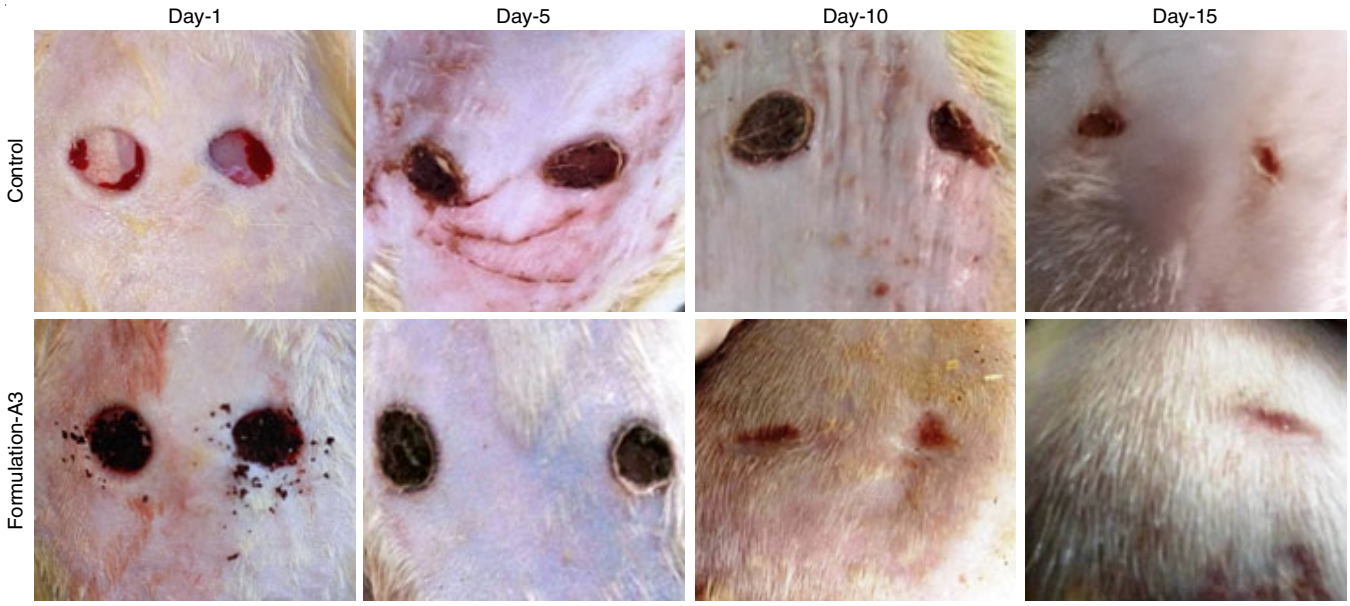

Fig. 9. Figure showing wound closure rate in 15 days

TABLE-3
RESULTS OF PERCENTAGE WOUND CLOSURE OF GEL FORMULATIONS

Time	Control		Gel formulation (A3)	
	Left wound	Right wound	Left wound	Right wound
Day-1	8.0	8.0	8.0	8.0
Day-5	8.0	8.0	6.0	5.5
Day-10	7.0	6.5	2.0	2.3
Day-15	4.5	2.0	–	0.5

group showed well-organized tissue architecture with intact epithelial layers, minimal inflammatory cell infiltration and well-formed granulation tissue. Collagen deposition appeared structured and aligned, reflecting a balanced extracellular matrix remodeling process. However, the positive group highlighted delayed wound healing due to minimal epithelialization (Fig. 10). This group was characterized by prominent inflammatory cell infiltration due to an extended inflammatory phase. Minimal collagen deposition and sparse fibroblast proliferation were also observed.

The formulation-A3 treated group showed very fast wound closure with prominent epithelial layers as compared to the positive group. This implies a shorter inflammatory phase with minimal inflammatory infiltration and higher density with pronounced collagen deposition along with increased fibroblast proliferation. Also, the presence of good granulation tissue formation with very minimal necrotic debris further underlines the better healing potential for formulation-A3. Furthermore, enhanced re-epithelialization and reduced inflammatory cell infiltration suggest that formulation-A3 promotes faster tissue repair by modulating the inflammatory response. This increase in proliferating fibroblasts and dense collagen deposition points toward the role of formulation-A3 in remodeling the extracellular matrix, which is pertinent to tissue integrity and wound contraction. Overall, formulation-A3 shows excellent wound healing potential by promoting rapid wound closure, reducing inflammation, promoting fibroblast proliferation and enhancing collagen synthesis. These results support the use of formulation-A3 as a promising candidate for wound care applications.

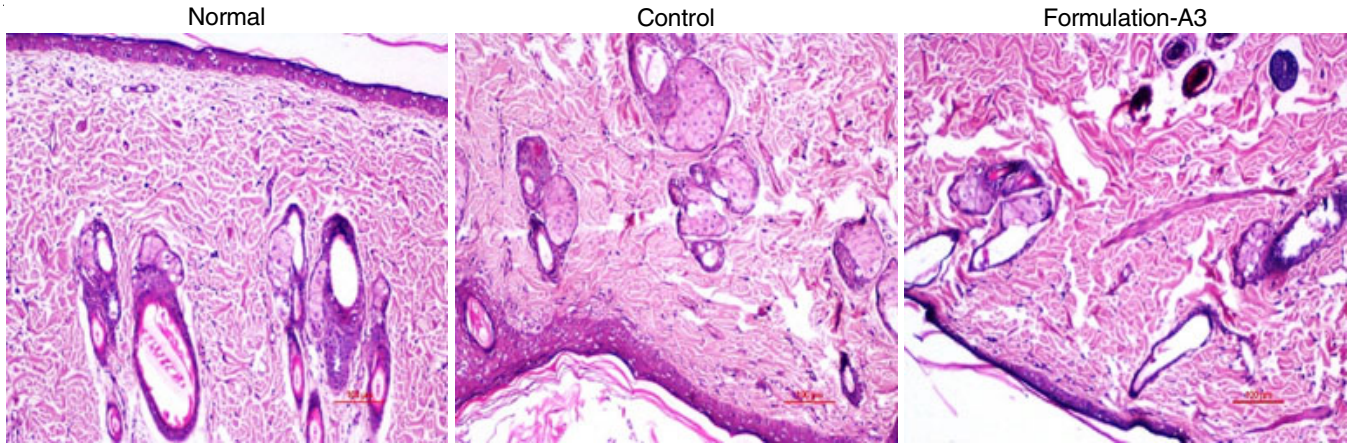

Fig. 10. Histopathology studies

Conclusion

This study effectively developed neem gum-gelatin biocomposites for sustained drug delivery in wound healing. The biocomposites, synthesized *via* pH-induced crosslinking, exhibited strong intermolecular interactions confirmed by FTIR, XRD and SEM analysis. Solid dispersions of clindamycin phosphate showed enhanced stability and controlled drug release over 24 h. The formulated topical gel established enviable physicochemical properties and superior antimicrobial activity against *E. coli* and *Micrococcus*, suggesting its potential in preventing infections. The *in vivo* studies confirmed accelerated wound healing, with enhanced wound closure rates and improved histopathological outcomes. Thus, based on the these findings, the neem gum-gelatin biocomposites as a biodegradable, biocompatible and cost-effective polymeric system for wound care were established.

ACKNOWLEDGEMENTS

The authors thankfully acknowledge the support and institutional facilities provided by Chitkara College of Pharmacy, Chitkara University, Punjab, India.

CONFLICT OF INTEREST

The authors declare that there is no conflict of interests regarding the publication of this article.

REFERENCES

1. S. Guo and L.A. DiPietro, *J. Dent. Res.*, **89**, 219 (2010); https://doi.org/10.1177/0022034509359125
2. S. Das, B. Mishra, K. Gill, M.S. Ashraf, A.K. Singh, M. Sinha, S. Sharma, I. Xess, K. Dalal, T.P. Singh and S. Dey, *Int. J. Biol. Macromol.*, **48**, 38 (2011); https://doi.org/10.1016/j.ijbiomac.2010.09.010
3. S. Dhivya, V.V. Padma and E. Santhini, *Biomedicine*, **5**, 22 (2015); https://doi.org/10.7603/s40681-015-0022-9
4. A. Sood, M.S. Granick and N.L. Tomaselli, *Adv. Wound Care*, **3**, 511 (2014); https://doi.org/10.1089/wound.2012.0401
5. T. Lagoa, M.C. Queiroga and L. Martins, *Pharmaceuticals*, **17**, 1110 (2024); https://doi.org/10.3390/ph17091110
6. K.P. Valente, A. Brolo and A. Suleman, *Molecules*, **25**, 507 (2020); https://doi.org/10.3390/molecules25030507
7. G. Suarato, R. Bertorelli and A. Athanassiou, *Front. Bioeng. Biotechnol.*, **6**, 137 (2018); https://doi.org/10.3389/fbioe.2018.00137
8. M. Ansari and A. Darvishi, *Front. Bioeng. Biotechnol.*, **12**, 1309541 (2024); https://doi.org/10.3389/fbioe.2024.1309541
9. M. Mir, M.N. Ali, A. Barakullah, A. Gulzar, M. Arshad, S. Fatima and M. Asad, *Progr. Biomater.*, **7**, 1 (2018); https://doi.org/10.1007/s40204-018-0083-4
10. R. Sadeghi, N. Ebrahimi and M.D. Tehrani, *Polymer*, **98**, 365 (2016); https://doi.org/10.1016/j.polymer.2016.06.050
11. B. Singh and K. Ram, *Results Surf. Interfaces*, **13**, 100161 (2023); https://doi.org/10.1016/j.rsurfi.2023.100161
12. T. Muthukumar, J.E. Song and G. Khang, *Molecules*, **24**, 4514 (2019); https://doi.org/10.3390/molecules24244514
13. R. Naomi, H. Bahari, P.M. Ridzuan and F. Othman, *Polymers*, **13**, 2319 (2021); https://doi.org/10.3390/polym13142319
14. H. Cao, J. Wang, Z. Hao and D. Zhao, *Front. Pharmacol.*, **15**, 1398939 (2024); https://doi.org/10.3389/fphar.2024.1398939
15. A. Hameed, T.U. Rehman, Z.A. Rehan, R. Noreen, S. Iqbal, S. Batool, M.A. Qayyum, T. Ahmed and T. Farooq, *Front. Mater.*, **9**, 1042304 (2022); https://doi.org/10.3389/fmats.2022.1042304
16. R. Malviya, *Precis. Med. Sci.*, **9**, 68 (2020); https://doi.org/10.1002/prm2.12025
17. S. Hua, *Int. J. Nanomed.*, **9**, 735 (2014); https://doi.org/10.2147/IJN.S55805
18. A. Sharma, V. Puri, P. Kumar and I. Singh, *Membranes*, **11**, 7 (2020); https://doi.org/10.3390/membranes11010007